

**HYGROTHERMAL EFFECTS ON THE DEFLECTION – INDUCED
VOLTAGE AND STRESSES IN COMPOSITE PIEZOELECTRIC
STRUCTURES**

**By
Hani Ahmad Al Daradkah**

**Supervisor
Dr. Naser Al Huniti, Prof.**

**This Thesis was submitted in Partial Fulfillment of the Requirements for the
Master's Degree of science in Mechanical Engineering**

**Faculty of Graduate Studies
The University of Jordan**

January, 2009

COMMITTEE DECISION

This Thesis (Hygrothermal Effects on the Deflection –Induced Voltage and Stresses in Composite Piezoelectric Structures) was Successfully Defended and Approved on 7 / 8 / 2008

Examination Committee

Signature

Dr. Saad Habali. (On behalf-Supervisor)
Prof. of Applied Mechanics


c. n. s. / 8 / 2008

Dr. Mazen Al-Qaisi (Member)
Prof. of Applied Mechanics


c. n. s. / 8 / 2008

Dr. Salih Akour (Member)
Assoc. Prof. Of Applied Mechanics


c. n. s. / 8 / 2008

Dr. Mousa Mohsen (Member)
Prof. of Applied Mechanics
(The Hashemite University)


Mousa Mohsen

تعتمد كلية الدراسات العليا
هذه النسخة من الرسالة
التوقيع.....التاريخ..... 7/8/2008

Dedication

To my family who support me to do my best with their
inspiration, courage, struggle, patience and endless love

Acknowledgement

Special recognition is given to my supervisor Prof. Naser Al-Huniti who introduced me to this amazing field and motivated me to work in this subject and is still inspiring me to go further in the field. My warm thanks to Prof. Saad Habali for his support and valuable time. Finally, I want to thank every person who gave me even a small help.

TABLE OF CONTENTS

Committee Decision	ii
Dedication	iii
Acknowledgement	iv
Table of contents	v
List of tables	vii
List of figures	viii
Nomenclature	xi
Abstract	xiii
1 INTRODUCTION	1
1.1 Introduction	1
1.2 Piezoelectric sensor	3
1.3 Composite materials	3
1.4 Hygrothermal Effects	4
1.5 Literature Review	6
1.6 Objectives	10
1.7 Thesis Overview	11
2 THEORETICAL FORMULATION	12
2.1 Lamination Theory	12
2.2 Governing Equations	12
2.2.1 Composite Beam	15
2.2.2 Piezoelectric Composite Beam	16
2.2.3 Hygrothermal Piezoelectric Composite Beam	18

3. FINITE ELEMENT METHOD	20
3.1 Introduction	20
3.2 Overview of ANSYS	20
3.3 Modeling of the present problem	21
3.4 Boundary Conditions	24
3.5 Meshing	25
4 RESULTS	26
4.1 Composite Beam	27
4.2 Piezoelectric Composite Beam	30
4.3 Hygrothermal Piezoelectric Composite Beam	33
4.3 Composite Plate	38
5 CONCLUSIONS AND RECOMMENDATIONS	45
5.1 Conclusions	45
5.2 Recommendations	45
References	46
Abstract (in Arabic)	48

LIST OF TABLES

Table: 5.1 Beam Parameters

38

LIST OF FIGURES

Figure 2.1 Composite beam loaded by a concentrated load	13
Figure 3.1 Solid 95	21
Figure 3.2 Composite Beam constrained at one end	22
Figure 3.3 Solid 226	23
Figure 3.4 Composite Plate constrained at two edges	24
Figure 4.1 Composite beam deflection	27
Figure 4.2 Composite beam horizontal deflection	27
Figure 4.3 Composite beam horizontal deflection curve	28
Figure 4.4 Composite beam vertical deflection	28
Figure 4.5 Composite beam vertical deflection curve	29
Figure 4.6 Composite beam stresses	29
Figure 4.7 Composite beam stresses curve	30
Figure 4.8 Piezoelectric composite beam horizontal deflection	30
Figure 4.9 Piezoelectric composite beam horizontal deflection curve	31
Figure 4.10 Piezoelectric composite beam vertical deflection	31
Figure 4.11 Piezoelectric composite beam vertical deflection curve	32
Figure 4.12 Piezoelectric composite beam stresses	32
Figure 4.13 Piezoelectric composite beam stresses curve	33
Figure 4.14 Piezoelectric composite beam induced voltage curve	33
Figure 4.15 Hygrothermal piezoelectric composite beam horizontal deflection	34
Figure 4.16 Hygrothermal piezoelectric beam horizontal deflection curve	34
Figure 4.17 Hygrothermal piezoelectric composite beam vertical deflection	35

Figure 4.18 Hygrothermal composite beam vertical deflection curve	35
Figure 4.19 Hygrothermal piezoelectric composite beam stresses	36
Figure 4.20 Hygrothermal piezoelectric composite beam stresses curve	36
Figure 4.21 Comparison between u values at different moisture values	36
Figure 4.22 Comparison between w values at different moisture values	37
Figure 4.23 Comparison between σ values at different moisture values	37
Figure 4.24 composite plate deflection	38
Figure 4.25 composite plate deflection (side view)	38
Figure 4.26 composite plate horizontal deflection	39
Figure 4.27 composite plate vertical deflection	39
Figure 4.28 composite plate stresses	39
Figure 4.29 composite plate horizontal deflection curve	40
Figure 4.30 composite plate vertical deflection curve	40
Figure 4.31 composite plate stresses curve	40
Figure 4.32 Piezoelectric composite plate horizontal deflection	41
Figure 4.33 Piezoelectric composite plate vertical deflection	41
Figure 4.34 Piezoelectric composite plate stresses	41
Figure 4.35 Piezoelectric composite plate horizontal deflection curve	42
Figure 4.36 Piezoelectric composite plate vertical deflection curve	42
Figure 4.37 Piezoelectric composite plate stresses curve	42
Figure 4.38 Hygrothermal piezoelectric composite plate horizontal deflection	43
Figure 4.39 Hygrothermal piezoelectric composite plate vertical deflection	44
Figure 4.40 Hygrothermal piezoelectric composite plate stresses	44

Figure 4.41 Hygrothermal piezoelectric plate horizontal deflection curve	45
Figure 4.42 Hygrothermal piezoelectric plate vertical deflection curve	45
Figure 4.43 Hygrothermal piezoelectric composite plate stresses curve	45

NOMENCLATURE

σ_{ij}	Stress tensor
Q_{ijkl}	Stiffness coefficients tensor
ε_{kl}	The strain tensor
α_{kl}	The thermal expansion coefficients tensor
β_{kl}	The hygroscopic tensor
E_k	The electric field vector
P_j	The pyroelectric vector
u, v, w	Displacements in x, y, and z directions respectively
u_o, v_o, w_o	Middle surface displacements
$\varepsilon_{xo}, \varepsilon_{yo}, \varepsilon_{xyo}$	Mid surface strains
$\kappa_x, \kappa_y, \kappa_{xy}$	The curvatures
N	Stress resultants
Q	Shear resultants
M	Stress couples
E	Modulus of elasticity
v	Poisson's ratio
G	Shear Modulus of elasticity
e	Piezoelectric coefficient
λ	Dielectric coefficient
m	Moisture Content
T_{gdr}	Glass transition temperature of dry resin

T	Temperature at which property to be measured
T ₀	Room temperature
T _{gwr}	Glass transition temperature of wet resin
V _f	Fiber Volume Fraction
h	Beam or Plate Height
L	Beam and Plate length
w	Beam or Plate width
C	Induced charge
V	Induced electric field potential of the PZT
c _p	Capacitance

HYGROTHERMAL EFFECTS ON THE DEFLECTION – INDUCED VOLTAGE AND STRESSES IN COMPOSITE PIEZOELECTRIC STRUCTURES

By
Hani Ahmad Al Daradkah

Supervisor
Dr. Naser Al-Huniti, Prof.

ABSTRACT

The main concern of the present work is the investigation of the piezoelectric response of structures that appears in the form of a relation between mechanical stress and electrical voltage that presents a form of coupling between the electrical and mechanical properties of a material. The investigation included the general response of piezoelectric beam and plate structures to hygrothermal loading. The interactions between voltage, deflections and stresses are investigated in these structures. Finite element technique is used to model the structures under consideration. Theoretical approximate solution is proposed based on the elastic analysis of the classical lamination theory.

Different cases of structures are studied based on two-dimensional linear theory of elasticity and piezoelectricity then same piezoelectric beam was studied under hygroscopic and thermal (hygrothermal) effects. Both the piezoelectric coefficient and the thickness for different layers are taken as variables. The solutions obtained in the present investigation are compared with numerical results from ANSYS software and same numerical results are obtained for composite plate and piezoelectric plate and hygrothermal piezoelectric plate. Different moisture contents are considered and compared.

1 INTRODUCTION

1.1 Introduction

Piezoelectric materials are solids that describe the relation between mechanical stress and electrical voltage. An applied mechanical stress will generate a voltage and an applied voltage will change the shape of the solid by a small amount. The piezoelectric effect is a phenomena resulting from coupling between the electrical and mechanical properties of a material. When mechanical stress is applied to a piezoelectric material, an electric potential will be produced. Likewise, when an electric potential is applied to the material a mechanical behavior will occur. Piezoelectric materials thus have numerous applications as electro-mechanical transducers which can convert electrical signals into mechanical motion and vice-versa.

Piezoelectric devices include different types like crystals, tubes, unimorphs, bimorphs and stacks. Piezoelectric crystals involve a non-uniform charge distribution within the unit cell of the crystal. When exposed to an electric field, this charge distribution shifts and the crystal will change its shape. The same polarization mechanism can cause a voltage to develop across the crystal in response to a mechanical force.

Piezo tubes are useful devices for fine control of an object in space. By sectioning the surface of a tube into four regions and connecting them, as well as one end of the tube to electrodes, it becomes possible to apply voltages to the tube in various directions. By applying voltages perpendicular to the tubes cross-section, it becomes possible to control the position of one end of the tube in two dimensions (x and y), while applying a voltage along the length of the tube, it becomes possible to control the position in the third dimension (z).

Because the force and displacement created by a pure piezoelectric material are relatively small, methods have been developed to allow amplification of the piezoelectric effect. One approach (known as a unimorph) is to apply a thin layer of a piezoelectric material to a layer of inactive material. When the piezo expands or contracts, the device will then bend in response. By combining more than one piezo, it becomes possible to further increase the amount of transduction. For instance, An elongating, bending or twisting device can be created by placing two layers of piezoelectric material on top of one-another, and by controlling the polarization direction and the voltages such that when one layer contracts, the other will expand. Such a device is known as a bimorph. By stacking of piezo materials into layers, it becomes possible to combine their displacement to create what is known as a piezo stack. Such devices are capable of higher displacements and larger forces.

An everyday life application example is the car's airbag sensor. The material detects the intensity of the shock and sends an electrical signal which triggers the airbag. Other commercial applications of piezoelectric devices abound, for instance in speakers, spark generators inside electronic igniters, strain sensors pressure gages, stress measurements, vibration measurements, sonar, and as precise time-keepers in electronic clocks.

The design of intelligent structures by combining piezoelectric layers in the composite laminates taking the advantage of their electromechanical properties has gained popularity among the researchers and designers.

Aerospace structures are typical examples of structures made of advanced composite materials that may be exposed to heat and moisture during their service life.

1.2 Piezoelectric sensor

Based on piezoelectric technology various physical quantities can be measured; the most common are pressure and acceleration. For pressure sensors, a thin membrane and a massive base are used, ensuring that an applied pressure specifically loads the elements in one direction. For accelerometers, a mass is attached to the crystal elements. When the accelerometer experiences a motion, the invariant mass loads the elements according to Newton's second law of motion.

The main difference in the working principle between these two cases is the way that forces are applied to the sensing elements. In a pressure sensor a thin membrane is used to transfer the force to the elements, while in accelerometers the forces are applied by an attached seismic mass.

Sensors often tend to be sensitive to more than one physical quantity. Pressure sensors show false signal when they are exposed to vibrations. Sophisticated pressure sensors therefore use acceleration compensation elements in addition to the pressure sensing elements. By carefully matching those elements, the acceleration signal (released from the compensation element) is subtracted from the combined signal of pressure and acceleration to derive the true pressure information.

1.3 Composite materials:

Composite materials are engineering materials made from two or more constituent materials to attain desired properties with significantly different physical or chemical properties and which remain separate and distinct on a macroscopic level within the finished structure.

Applications of composites include aircraft, aerospace industry, automobile industry and building structures.

Most composites are made up of just two materials. One material (the matrix or binder) surrounds and binds together a cluster of fibers or fragments of a much stronger material (the reinforcement). In the case of mud bricks, the two roles are taken by the mud and the straw; in concrete, by the cement and the aggregate. In fiberglass, the reinforcement is provided by fine threads or fibers of glass, often woven into a sort of cloth, and the matrix is a plastic.

The analysis of such structures is a complex task, compared with conventional single layer metallic structures, because of the exhibition of coupling among membrane, torsion and bending strains; weak transverse shear rigidities; and discontinuity of the mechanical characteristics along the thickness of the laminates. For these reasons, in recent years, there is a great deal of research interest for accurately modeling and simulating the characteristics of composite structures through different higher order displacement functions for two-dimensional theories as they lead to less expensive models compared to three-dimensional one.

The design of intelligent structures by combining piezoelectric layers in the composite laminates taking the advantage of their electromechanical properties has gained popularity among the researchers and designers.

1.4 Hygrothermal Effects:

The use of fiber reinforced matrix composites in engineering applications has been tremendously increasing. Therefore, it is very important to study the response of these materials to environmental conditions like temperature and moisture. The performance of

these materials degrades as a result of hygrothermal exposure. Due to moisture and temperature exposure, properties such as the stiffness, strength, life, modulus and conductivities of a composite material decrease considerably. Therefore, experimental and analytical methods have to be carried out to study their responses.

Structures made of advanced composite materials may be exposed to thermal and hygroscopic (moisture) effects during their service life.

Hygrothermal effects can reduce the stiffness of the structural systems and influence actuating and sensing behavior of piezoelectric materials.

Also, thermal stresses may cause damage and dynamic instability.

Prolonged exposure to a hygrothermal environment has two major effects on a composite structure. The first one is of a residual nature. The coefficient of thermal expansion is usually higher for the matrix. Polymers absorb moisture readily whereas fibers are hardly affected by a wet environment. Further the absorption of moisture by the matrix is more pronounced at higher temperatures. An increase in the ambient temperature and/or humidity level causes the matrix to expand; contrarily, reduced temperature and/or moisture level of the surrounding environment results in a contraction of the matrix. Since the fibers are relatively unaffected to changes in temperature and moisture content, the differential expansion/contraction leads to residual stresses in the matrix laminates. These residual stresses may starkly reduce the load carrying capacity of a structure made of a polymer matrix composite.

The second significant effect of an increased hygrothermal condition is the degradation of the mechanical properties of the matrix material. The degradation occurs in

both the stiffness and strength values of the matrix and consequently in the corresponding values of the lamina.

1.5 Literature Review

Although a good amount of research work has been published on piezoelectric structures, very few investigations have studied effects of hygrothermal loading on these structures. Such investigations were concerned with delamination, buckling and natural frequencies, in addition to the control of hygrothermal effect.

Chen et. al. (2007) proposed the vibration analysis of an asymmetric composite beam composed of glass piezoelectric material. The Bernoulli's beam theory is adopted for mechanical deformations, and the electric potential field of the piezoelectric material is assumed such that the divergence-free requirement of the electrical displacements is satisfied. The accuracy of the analytic model is assessed by comparing the resonance frequencies obtained by the analytic model with those obtained by the finite element method. The model developed can be used as a tool for designing piezoelectric actuators such as micro-pumps.

Chien et. al. (2006) proposed a novel piezoelectric cantilever bimorph micro transducer electro-mechanical energy conversion model. The coupling between the mechanical strain and the piezoelectric polarization was used to deduce the vibration-induced voltage and electrical energy in this new piezoelectric-base power generator model. The analytical model shows that the vibration-induced voltage is proportional to the excitation frequency of the device but inversely proportional to the length of cantilever beam and the damping factor. To verify the theoretical analysis, two micro transducer

clusters were fabricated. The experimental results demonstrated that the maximum output voltage deviated very little from the analytical model.

Shi et. al. (2006) studied Both multi-layer piezoelectric cantilevers and multi-layer piezoelectric composite cantilevers based on 2D linear theory of elasticity and piezoelectricity. Both the piezoelectric coefficient and the thickness for different layers are taken as variables and the investigation gives exact solutions for the variation of these parameters by introducing several recurrence formulae. This work shows that the properties of some typical piezoelectric cantilever models can be directly obtained as some special cases of this investigation

Panda and Pradhan (2006) proposed two sets of full three-dimensional thermoelastic finite element analyses of superimposed thermo-mechanically loaded composite laminates. Residual stresses developed due to the thermoelastic anisotropy of the laminae are found to strongly influence the delamination onset and propagation characteristics, which have been reflected by the asymmetries in the nature of energy release rate plots and their significant variation along the delamination front.

Tan and Tong (2006) proposed one-dimensional analytical model to investigate the non-linear behavior for piezoelectric and piezoelectric fiber reinforced composite (PFRC) materials in the fiber direction. A numerical results reveal a significant effect of stress on Strain–Electric Field non-linear behavior for both soft piezoelectric ceramics and piezoelectric crystals.

Huang and Liu (2006) proposed the fully coupled response characteristics of a multilayered composite plate with piezoelectric layers. The response quantities of the plate are coupled by the mechanical field and the electric field. Numerical results show that the

plate aspect ratio, plate thickness ratio, lamination scheme, fiber orientations, and piezoelectric coupling significantly influence the static and dynamic responses of the plate.

Praveen Kumar Kavipurapu (2005) the dynamic response of simply supported glass/epoxy composite beams subjected to moving loads in a hygrothermal environment is carried out using the general purpose finite element program *ANSYS*. The moving load model and the hygrothermal incorporation are validated separately by reproducing results available in the literature. The hygrothermal effect is introduced by using empirical relations for degrading the material stiffness properties of the matrix.

Cheng et. al. (2005) considered the effects of both the different material properties of composite layers and the poling directions of piezoelectric layers. They utilized the assumption of the simple-higher-order shear deformation theory to model and analyze the laminated composite plate integrated with the random poled piezoelectric layers. Based on Hamilton's variation principle for electro-elasticity, the generalized governing equations and relative boundary conditions for the anisotropic piezoelectric/composite laminate plate were carried out on the assumption of Reddy's simple high-order theory.

Raja et. al. (2004) present the influence of active stiffness on the dynamic behaviour of piezo-hygro-thermo-elastic laminates. A coupled piezoelectric finite element formulation involving a hygrothermal strain field is derived using the virtual work principle and is employed in a nine-noded field consistent Lagrangian element. The hygrothermal strain modifies the elastic stiffness and brings down the elastic frequencies of piezoelectric laminated plates and shells significantly. The active stiffening and active compensation effects are low in moderately thick piezo-hygro-thermo-elastic plates and shells, which are less influenced by boundary conditions.

Datchanamourty (2004) develops a mixed finite element model for composite plates. Dynamic and coupled piezoelectric effects on the nonlinear bending of plates are investigated. Upon the completion of the analysis of piezoelectric plates, the two-dimensional composite plate theory will be extended to plate structures. Lagrangian hierarchic finite elements are used to model the plates.

Schultz (2003) develops a model to predict the snap-through behavior of simple, rectangular, two layer, unsymmetric cross-ply laminates actuated with piezoelectric actuators. Then this model used to design an experiment where snap through of such an unsymmetric laminate could be effected with a piezoelectric actuator, and to perform the designed experiment to compare with the developed model.

Song et. al. (2003) proposed the surface shape of precision structures such as spacecraft antenna reflectors. This paper presents numerical and experimental results of active compensation of thermal deformation of a composite beam using piezoelectric ceramic actuators. experiments are conducted to study the thermal effect, the piezoelectric actuation effect and active thermal distortion compensation using piezoelectric actuators with a proportional, integral and derivative feedback controller.

Patel et. al. (2002) studied static and dynamic characteristics of thick composite laminates exposed to hygrothermal environment using a realistic higher-order theory developed recently. The study, here, has been focused on the effects of different moisture concentrations/temperature in the plates, in predicting the structural behavior of composite laminates. The effects of various terms in the higher-order displacement model in predicting the responses such as deflection, buckling load and natural frequencies of laminates subjected to the exposure of hygrothermal environment are discussed.

Cheung and Jiang (2001) developed two kinds of the finite layer method in three dimensional analysis of rectangular composite laminates with actuator and sensor layers (piezoelectric materials). The generalized displacement functions are constructed, and the generalized stiffness matrices are derived in explicit form, which are especially convenient for application in engineering. Numerical examples are presented and compared with available results to demonstrate the efficiency and accuracy of the present method.

Wang and Noda (2001) discussed the fracture behavior of the cracked smart actuator on a substrate under thermal load. The actuator is made of piezoelectric material with functionally graded material (FGM) properties. Crack initiation angle were determined from the location of minimum energy density factors.

Tan and Tong (2001) proposed two non linear micromechanics models for predicting the non linear behavior of unidirectional PFRC material, which are subjected to a high monotonic electric field. The required closed-form formulas for the effective electroelastic constants of PFRC materials are obtained using the non-linear constitutive equations for purely piezo-electric materials and the iso-field assumptions. The single and double loading conditions are introduced when deriving these closed form formulas.

1.6 Objectives:

- To investigate the behavior of a piezoelectric composite beam and plate in the presence of thermal and hygroscopic effects using ANSYS software. The main concern is the effect of these conditions on the deflection-induced voltage in the structure and the resulting stresses.
- To apply analytical procedure to model and solve the same beam.

- In the present research only the degradation effect of the mechanical properties is considered while ignoring the residual stresses.

1.7 Thesis Overview:

Chapter Two explains the theory of the present study in addition to the formulation of governing equations for hygrothermal piezoelectric composite beam and plate.

In chapter Three the finite element modeling of Hygrothermal Piezoelectric Composite Beam in *ANSYS* is detailed.

Chapter Four presents the results obtained in the present study. The graphs obtained from *ANSYS* program and analytical procedure are attached here.

Chapter Five has the conclusions of the present study and recommendations for the future work.

2 THEORETICAL FORMULATION

2.1 Lamination Theory:

The lamination theory deals with the elastic response of laminates subjected to in-plane forces, bending moments, in addition to thermal and hygroscopic loading. The theory is used to predict the effective engineering properties, typical stress distributions, and through-thickness Poisson's ratios and coefficients of thermal expansion.

The following assumptions are fundamental to lamination theory:

- The laminate consists of perfectly bonded layers (Laminae)
- Each layer is made of a homogeneous material with known effective properties
- Individual layer properties can be isotropic (whose properties are independent of direction and whose planes are all planes of symmetry), orthotropic (which has three mutually perpendicular planes of symmetry), or transversely isotropic (whose effective properties are isotropic in one of the planes).
- Each layer is in a state of plane stress

2.2 Governing Equations:

Consider the laminated beam shown in Figure 2.1.

| z

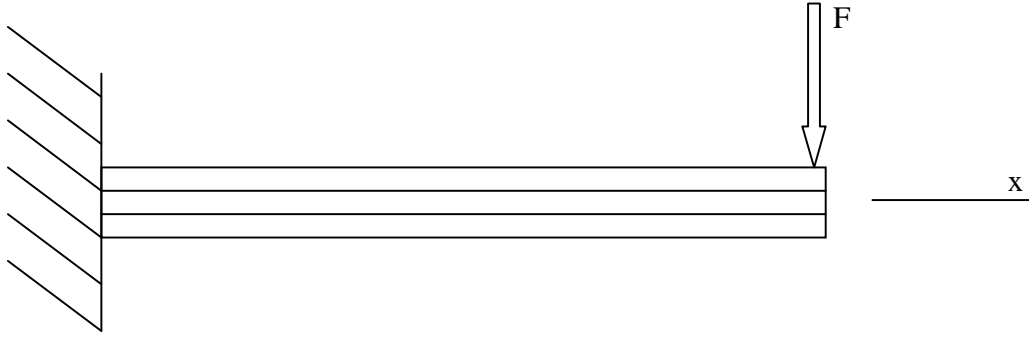


Figure 2.1 Composite beam loaded by a concentrated load

The constitutive equations of a piezo-hygro-thermo-elastic composite lamina can be expressed as:

$$\sigma_{ij} = Q_{ijkl} (\varepsilon_{kl} - \alpha_{kl} T - \beta_{kl} m) - e_{kij} E_k \quad (2.1)$$

Where σ_{ij} is the stress tensor, Q_{ijkl} is the stiffness coefficients tensor, ε_{kl} is the strain tensor, α_{kl} is the thermal expansion coefficients tensor, β_{kl} is the hygroscopic tensor, T is the temperature, m is the moisture content, e_{kij} is the piezoelectric coefficients tensor, and E_k is the electric field vector. On the other hand, the electric displacement vector (D_j) can be expressed as:

$$D_j = e_{jkl} \varepsilon_{kl} + \lambda_{jk} E_k + P_j T \quad (2.2)$$

where λ_{jk} is the dielectric coefficient tensor and P_j is the pyroelectric vector.

For orthotropic material and considering the fiber as the piezoelectric material, the constitutive equations can be written in matrix form as follows:

$$\begin{Bmatrix} \sigma_1 \\ \sigma_2 \\ \sigma_3 \\ \sigma_4 \\ \sigma_5 \\ \sigma_6 \end{Bmatrix} = \begin{bmatrix} Q_{11} & Q_{12} & Q_{13} & 0 & 0 & 0 \\ Q_{12} & Q_{22} & Q_{23} & 0 & 0 & 0 \\ Q_{13} & Q_{23} & Q_{33} & 0 & 0 & 0 \\ 0 & 0 & 0 & 2Q_{44} & 0 & 0 \\ 0 & 0 & 0 & 0 & 2Q_{55} & 0 \\ 0 & 0 & 0 & 0 & 0 & 2Q_{66} \end{bmatrix} \begin{Bmatrix} \varepsilon_1 - \alpha_1 \Delta T - \beta_1 \Delta m \\ \varepsilon_2 - \alpha_2 \Delta T - \beta_2 \Delta m \\ \varepsilon_3 - \alpha_3 \Delta T - \beta_3 \Delta m \\ \varepsilon_{23} \\ \varepsilon_{31} \\ \varepsilon_{12} \end{Bmatrix} = \begin{bmatrix} 0 & 0 & 0 \\ 0 & 0 & e_{32} \\ 0 & 0 & e_{33} \\ 0 & e_{23} & 0 \\ e_{13} & 0 & 0 \\ 0 & 0 & 0 \end{bmatrix} \begin{Bmatrix} E_1 \\ E_2 \\ E_3 \end{Bmatrix} \quad (2.3)$$

$$\begin{Bmatrix} D_1 \\ D_2 \\ D_3 \end{Bmatrix} = \begin{bmatrix} 0 & 0 & 0 & 0 & e_{13} & 0 \\ 0 & 0 & 0 & e_{23} & 0 & 0 \\ 0 & e_{32} & e_{33} & 0 & 0 & 0 \end{bmatrix} \begin{Bmatrix} \varepsilon_1 \\ \varepsilon_2 \\ \varepsilon_3 \\ \varepsilon_{23} \\ \varepsilon_{31} \\ \varepsilon_{12} \end{Bmatrix} + \begin{bmatrix} \lambda_1 & 0 & 0 \\ 0 & \lambda_2 & 0 \\ 0 & 0 & \lambda_3 \end{bmatrix} \begin{Bmatrix} E_1 \\ E_2 \\ E_3 \end{Bmatrix} \quad (2.4)$$

where:

$$\begin{aligned}
 Q_{11} &= E_{11}(1 - \nu_{23}\nu_{32})/\Delta & , & & Q_{22} &= E_{22}(1 - \nu_{31}\nu_{13})/\Delta \\
 Q_{33} &= E_{33}(1 - \nu_{12}\nu_{21})/\Delta & , & & Q_{44} &= G_{23} \\
 Q_{55} &= G_{13} & , & & Q_{66} &= G_{12} \\
 Q_{12} &= E_{11}(\nu_{23} + \nu_{31}\nu_{23})/\Delta & , & & Q_{13} &= E_{11}(\nu_{31} + \nu_{21}\nu_{32})/\Delta \\
 Q_{23} &= E_{22}(\nu_{32} + \nu_{12}\nu_{31})/\Delta \\
 \Delta &= 1 - \nu_{12}\nu_{21} - \nu_{23}\nu_{32} - \nu_{31}\nu_{13} - 2\nu_{21}\nu_{32}\nu_{13} \quad (2.5)
 \end{aligned}$$

$$\begin{aligned}
 \nu_{ij} &= -\varepsilon_{ij} / \varepsilon_{ii} & , & & E_i &= \sigma_i / \varepsilon_i \\
 G_i &= E_i / 2(1 + \nu_i) \quad (2.6)
 \end{aligned}$$

where:

- ν : Poisson's ratio
 E : Modulus of elasticity

G : Shear Modulus of elasticity

2.2.1 Composite Beam:

For a composite beam without piezoelectric and hygrothermal effects the constitutive equations can be written as follows:

$$\begin{aligned}\varepsilon_x &= S_{11}\sigma_x + S_{13}\sigma_z \\ \varepsilon_z &= S_{13}\sigma_x + S_{33}\sigma_z \\ \varepsilon_{xz} &= S_{44}\sigma_{xz}\end{aligned}\quad (2.7)$$

For an elastic body the strain-displacement equations are given by:

$$\varepsilon_{ij} = \frac{1}{2}(u_{i,j} + u_{j,i}) \quad (2.8)$$

where $i,j=x,y,z$ in a Cartesian coordinate frame. Explicitly, the relations are:

$$\varepsilon_x = \frac{\partial u}{\partial x}, \quad \varepsilon_z = \frac{\partial w}{\partial z}, \quad \varepsilon_{xz} = \frac{1}{2}\left(\frac{\partial u}{\partial z} + \frac{\partial w}{\partial x}\right) \quad (2.9)$$

where u and w are the displacements in x and z directions respectively.

Neglecting body forces, the equilibrium equations for elastic materials can be given as:

$$\frac{\partial \sigma_x}{\partial x} + \frac{\partial \sigma_{xz}}{\partial z} = 0, \quad \frac{\partial \sigma_{xz}}{\partial x} + \frac{\partial \sigma_z}{\partial z} = 0 \quad (2.10)$$

To ensure that the displacement can be obtained by integrating equations (2.9), the components of strain must satisfy a set of compatibility equations as follows:

$$\frac{\partial^2 \varepsilon_x}{\partial z^2} + \frac{\partial^2 \varepsilon_z}{\partial x^2} = \frac{\partial^2 \varepsilon_{xz}}{\partial x \partial z} \quad (2.11)$$

In order to find the solution of the basic equations, the Airy stress function approach can be used. The stress function φ is introduced so that the components of stress can be expressed as:

$$\sigma_x = \frac{\partial^2 \varphi}{\partial^2 z}, \quad \sigma_z = \frac{\partial^2 \varphi}{\partial^2 x}, \quad \sigma_{xz} = -\frac{\partial^2 \varphi}{\partial x \partial z} \quad (2.12)$$

Furthermore, the stress function is assumed as:

$$\varphi = -az^3 + bz \quad (2.13)$$

where a and b are constants to be determined. The components of stress can be expressed as:

$$\sigma_x = -6az + 2b, \quad \sigma_z = \sigma_{xz} = 0 \quad (2.14)$$

From equations (2.7) and (2.14), it is easily verified that equation (2.11) is satisfied.

Further, by the use of equations (2.7) and (2.9), the displacements can be expressed as follows:

$$\begin{aligned} u &= -6aS_{11}xz + 2bS_{11}x + w_0z + u_0 \\ w &= -3aS_{13}z^2 + 2bS_{13}z + 3aS_{11}x^2 - w_0x + w_0 \end{aligned} \quad (2.15)$$

where u_0 and w_0 are constants to be determined by the use of geometrical conditions.

Equation (2.15) can be solved using the following boundary conditions:

$$\begin{aligned} w(0) &= 0, & w'(0) &= 0 \\ w(L) &= -\frac{PL^3}{3EI}, & w'(L) &= -\frac{PL^2}{2EI} \end{aligned} \quad (2.16)$$

2.2.2 Piezoelectric Composite Beam:

For piezoelectric composite beam (without hygrothermal effects) the constitutive equations can be written as follows:

$$\begin{aligned} \varepsilon_x &= S_{11}\sigma_x + S_{13}\sigma_z + g_{31}D_z \\ \varepsilon_z &= S_{13}\sigma_x + S_{33}\sigma_z + g_{33}D_z \\ \varepsilon_{xz} &= S_{44}\sigma_{xz} + g_{15}D_x \\ E_x &= -g_{15}\sigma_{xz} + \xi_{11}D_x \\ E_z &= -g_{31}\sigma_x - g_{33}\sigma_z + \xi_{33}D_z \end{aligned} \quad (2.17)$$

For piezoelectric materials, there is a set of geometric equations between the electric field and the electric potential ϕ , given as:

$$\begin{aligned}
 E_x &= -\frac{\partial\phi}{\partial x}, & E_z &= -\frac{\partial\phi}{\partial z} \\
 \varepsilon_x &= \frac{\partial u}{\partial x}, & \varepsilon_z &= \frac{\partial w}{\partial z}, & \varepsilon_{xz} &= \frac{1}{2}\left(\frac{\partial u}{\partial z} + \frac{\partial w}{\partial x}\right)
 \end{aligned} \tag{2.18}$$

Neglecting body charges, the induction components in the piezoelectric material should satisfy the following equilibrium equation:

$$\begin{aligned}
 \frac{\partial D_x}{\partial x} + \frac{\partial D_z}{\partial z} &= 0 \\
 \frac{\partial \sigma_x}{\partial x} + \frac{\partial \sigma_{xz}}{\partial z} &= 0, & \frac{\partial \sigma_{xz}}{\partial x} + \frac{\partial \sigma_z}{\partial z} &= 0
 \end{aligned} \tag{2.19}$$

To ensure that the displacement and electric potential can be obtained by integrating equations (2.18), the components of strain and electric field must satisfy a set of equations as follows:

$$\frac{\partial^2 \varepsilon_x}{\partial z^2} + \frac{\partial^2 \varepsilon_z}{\partial x^2} = \frac{\partial^2 \varepsilon_{xz}}{\partial x \partial z}, \quad \frac{\partial E_x}{\partial x} - \frac{\partial E_z}{\partial z} = 0 \tag{2.20}$$

In order to find the solution of the basic equations, the Airy stress function approach is used. The stress function φ and the induction function ψ is introduced so that the components of stress and induction can be expressed as:

$$\begin{aligned}
 \sigma_x &= \frac{\partial^2 \varphi}{\partial z^2}, & \sigma_z &= \frac{\partial^2 \varphi}{\partial x^2}, & \sigma_{xz} &= -\frac{\partial^2 \varphi}{\partial x \partial z} \\
 D_x &= \frac{\partial \psi}{\partial z}, & D_z &= \frac{\partial \psi}{\partial x}
 \end{aligned} \tag{2.21}$$

Further the stress function and induction function are assumed as:

$$\varphi = -az^3 + bz \quad \psi = cx \quad (2.22)$$

where a, b and c are constants to be determined. Further, the components of stress and induction can be expressed as:

$$\begin{aligned} \sigma_x &= -6az + 2b, & \sigma_z &= \sigma_{xz} = 0 \\ D_x &= 0 & D_z &= -c \end{aligned} \quad (2.23)$$

From equations (2.17) and (2.23), it is easily verified that equation (2.20) is satisfied. Further, by the use of equations (2.17) and (2.20), the displacements and electrical potential can be expressed as follows:

$$\begin{aligned} u &= -6aS_{11}xz + 2bS_{11}x + w_0z + u_0 \\ w &= -3aS_{13}z^2 + 2bS_{13}z + 3aS_{11}x^2 - w_0x + w_0 \\ \phi &= -3ag_{31}z^2 + 2bg_{31}z + \xi_{33}cz + \phi_0 \end{aligned} \quad (2.24)$$

where u_0 , w_0 and ϕ_0 are constants to be determined by the use of geometrical and electrical conditions.

Equation (2.15) can be solved using the following boundary conditions:

$$\begin{aligned} w(0) &= 0, & w'(0) &= 0 \\ w(L) &= -\frac{PL^3}{3EI}, & w'(L) &= -\frac{PL^2}{2EI} \\ \phi(0) &= 0, & \phi(h) &= V_0 \end{aligned} \quad (2.25)$$

2.2.3 Hygrothermal Piezoelectric Composite Beam:

For hygrothermal piezoelectric composite beam the same constitutive equations (2.17) can be written and the displacements and electrical potential can be expressed as follows:

$$\begin{aligned}
u &= -6aS_{11}xz + 2bS_{11}x + w_0z + u_0 \\
w &= -3aS_{13}z^2 + 2bS_{13}z + 3aS_{11}x^2 - w_0x + w_0 \\
\phi &= -3ag_{31}z^2 + 2bg_{31}z + \xi_{33}cz + \phi_0
\end{aligned} \tag{2.26}$$

where u_0 , w_0 and ϕ_0 are constants to be determined by the use of geometrical and electrical conditions.

Equation (2.26) can be solved using the following boundary conditions:

$$\begin{aligned}
w(0) &= 0, & w'(0) &= 0 \\
w(L) &= -\frac{PL^3}{3EI}, & w'(L) &= -\frac{PL^2}{2EI} \\
\phi(0) &= 0, & \phi(h) &= V_0
\end{aligned} \tag{2.27}$$

The stiffness properties of the constituents are degraded by using the empirical relations proposed by Chamis (1983) as shown:

$$\frac{P_{HTM}}{P_0} = \left[\frac{T_{gwr} - T}{T_{gdr} - T_0} \right]^{0.5} \tag{2.28}$$

where P is the property to be measured, HTM stands for hygrothermal mechanical, T_{gwr} is glass transition temperature of wet resin and T_{gdr} is the glass transition temperature of dry resin. T is the temperature at which property to be measured and T_0 is the room temperature. This is a steady state equation that relates the properties of the matrix for dry and wet conditions at particular values of moisture content and temperature.

The relation between T_{gdr} and T_{gwr} in terms of moisture content is given by Chamis and is stated as:

$$T_{gwr} = (0.005m^2 - 0.1m + 1.0)T_{gdr} \tag{2.29}$$

It is assumed that only matrix properties are affected by temperature change and moisture content. By using the rule of mixtures and changed properties of the matrix, updated elastic constants of the lamina and the laminate are calculated

3. FINITE ELEMENT METHOD

3.1 Introduction

Finite element analysis (FEA) is a computer simulation technique used in engineering analysis. It uses a numerical technique called the finite element method (FEM). In this technique, a mathematical/computer model of the structure is created and analyzed for deformations and stresses.

The model is divided into small blocks called elements. These elements are connected by nodes at which the finite element boundary conditions are applied. A set of algebraic equations are created for each element and combined simultaneous equations are solved. A post processor to the finite element program may be helpful in displaying the stresses and deflections in the form of contours for easy comprehension. A number of finite element packages are available for the analysis of complex structures under various types

of loads. A finite element package is chosen depending on the complexity of the model and the results needed.

3.2 Overview of ANSYS

ANSYS is one of the world's leading engineering simulation software providers. It develops general-purpose finite element analysis and computational fluid dynamics software. ANSYS develops a complete range of computer-aided engineering (CAE) products, but it is perhaps best known for its ANSYS Mechanical and ANSYS Multiphysics products.

ANSYS Mechanical and ANSYS Multiphysics software are self-contained analysis tools incorporating pre-processing (geometry creation, meshing), solver and post-processing modules in a unified graphical user interface. These are general-purpose finite element modeling packages for numerically solving a wide variety of mechanical problems, including static/dynamic structural analysis (both linear and non-linear), heat transfer and fluid problems, as well as acoustic and electro-magnetic problems.

The software is used to analyze a broad range of applications. ANSYS Mechanical technology incorporates both structural and material non-linearities. ANSYS Multiphysics software includes solvers for

thermal, structural, CFD, electromagnetics, and acoustics and can couple these separate physics together in order to address multidisciplinary applications. ANSYS software is also used in Civil Engineering, Electrical Engineering, Physics and chemistry.

3.3 Modeling of the present problem

In the present analysis Solid 95 element is used in this study as shown in figure (3.1). The Solid 95 element is a twenty-node layered structural solid mass element. This element has three degrees of freedom at each node, namely, translation in the X , Y , Z directions. This element can take a maximum of 100 layers and a user input option is available if more than 100 layers have to be modeled.

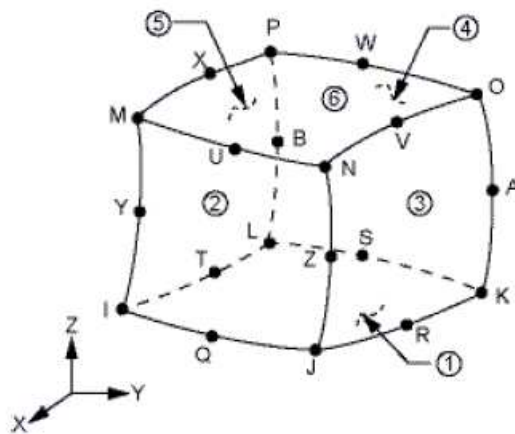


Figure 3.1 Solid 95

The simple beam is modeled with 500 elements (because the change is almost zero when using higher number of elements), one end is constrained at all DOF and the other end is free. The material properties of the beam are entered in the form of modulus of rigidity, Poisson's ratio and young's modulus.

Modeling of a beam made of composite material is a difficult task. Special attention has to be paid in defining the material properties, orientations of the layers and the element coordinate systems. The Solid 95 element is used in this study. Figure 3.2 shows description of a Solid 95 three layers composite element.

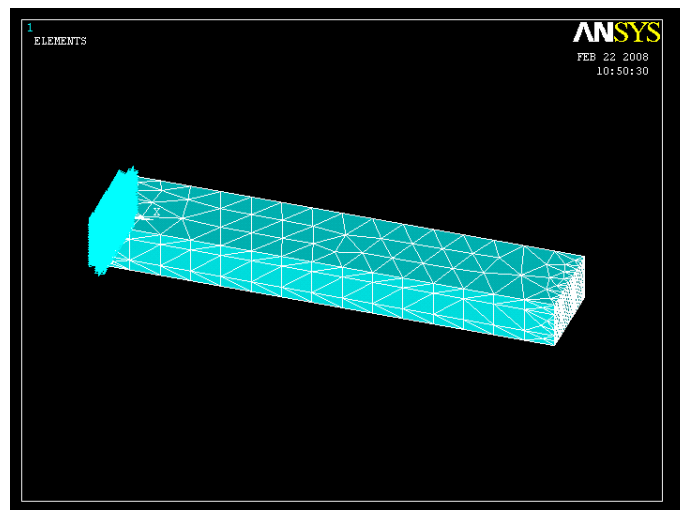


Figure 3.2 Composite Beam constrained at one end

Modeling of a piezoelectric composite beam is also consist of three layers. In the middle is the piezoelectric layer (Fiber) and in the upper and lower layers is the beam layers (Matrix). The material properties of

the piezoelectric layer are entered in the form of density, anisotropic elastic (stiffness matrix), orthotropic permittivity (dielectric coefficient) and piezoelectric matrix. The Solid 226 element (3-D 20 node coupled field solid with up to five degrees of freedom per node). SOLID226 shown in figure (3.2) is used in defining piezoelectric layer and Solid 95 is used in defining beam layers.

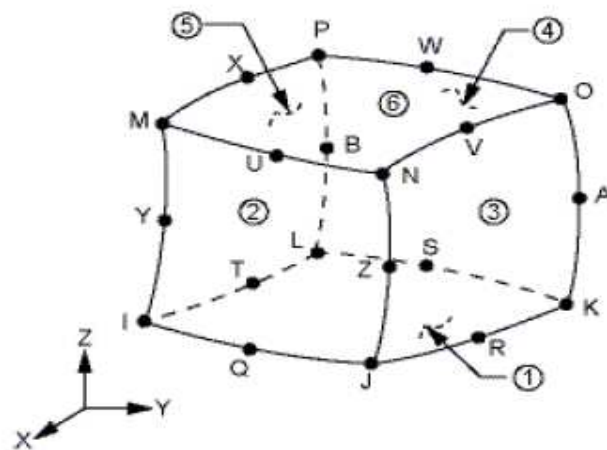


Figure 3.3 Solid 226

The response of laminated piezoelectric composite beams to hygrothermal conditions is studied to validate the hygrothermal aspect of the model. In this study, the stiffness properties of the constituents are degraded by using the empirical relations proposed by Chamis and explained in the previous chapter.

Same procedure can be applied to composite plate which modeled with 1200 elements (because the change is almost zero when using higher number of elements), two edges are constrained at all DOF and the other edges are free. The material properties of the plate are entered in the form of modulus of rigidity, Poisson's ratio and young's modulus.

Solid 95 element also used in this study. Figure 3.4 shows modeling of composite plate constrained at two edges.

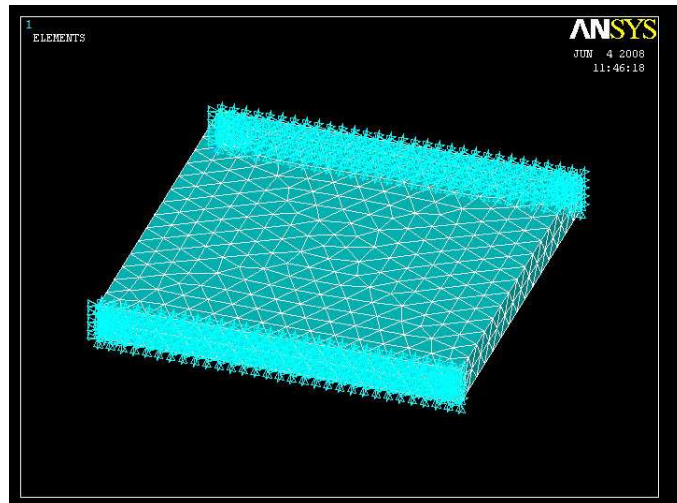


Figure 3.4 Composite Plate constrained at two edges

Modeling of a piezoelectric composite plate is also consist of three layers. In the middle is the piezoelectric layer (Fiber) and in the upper and lower layers is the beam layers (Matrix). The material properties of the piezoelectric layer are entered in the form of density, anisotropic elastic (stiffness matrix), orthotropic permittivity (dielectric coefficient)

and piezoelectric matrix. The Solid 226 element also used in defining piezoelectric layer and Solid 95 is used in defining beam layers.

The response of laminated piezoelectric composite plate to hygrothermal conditions is studied to validate the hygrothermal aspect of the model. Again, the stiffness properties of the constituents are degraded by using the empirical relations proposed by Chamis (1983).

3.4 Boundary Conditions

Boundary Conditions are the constraints and loads that can simulate the effect of the environment surrounding a body. Loads are applied in the form of forces, moments, pressures, temperatures, and moisture. The displacement constraints are applied by restricting the degrees of freedom at the corresponding nodes of a model. In the present research, simply supported plates and cantilevered beams are used for analysis.

3.5 Meshing

Meshing is the process of dividing the model into elements, which are connected by nodes at the element boundaries. Meshing is one of the important steps in successfully performing a finite element analysis. The type and density of the mesh determines the economy and accuracy of the solution. Therefore, an analyst should use valid assumptions in determining the exact meshing parameters. A coarse mesh can lead to inaccurate solutions and a very fine mesh may increase the time of

analysis. In order to define a suitable mesh, an analyst should have an idea of the parameter distributions within the model. Also a convergence study needs to be carried out by increasing the number of elements.

4 RESULTS

Table (4.1) lists the data of the elastic, piezoelectric, hygrothermal properties values. The material constants used in the calculations are determined from table (4.1) based on the constitutive equations, considering that most of the piezoelectric beams used in engineering fall under the plane strain condition.

Table: 4.1 Beam Parameters

Property	Value
Longitudinal Modulus, E_{11}	0.62E6 Pa
Transverse Modulus, E_{11}	0.62E6 Pa
Inter laminar Modulus, E_{11}	0.62E6 Pa
Major in-plane Poisson's ratio, ν_{12}	0.34
Out of plane Poisson's ratio, ν_{23}	0.34
Out of plane Poisson's ratio, ν_{13}	0.34
Longitudinal Shear Modulus, G_{12}	0.23E6 Pa
Inter Laminar Shear Modulus, G_{23}	0.23E6 Pa
Transverse Shear Modulus, G_{13}	0.23E6 Pa
Piezoelectric coefficients, e_{32}	-7.209
Piezoelectric coefficients, e_{33}	15.118
Piezoelectric coefficients, e_{23}	12.322
Piezoelectric coefficients, e_{13}	12.322
Dielectric coefficient, λ_1	804.6
Dielectric coefficient, λ_2	659.7
Dielectric coefficient, λ_3	804.6
Glass transition temperature of dry resin, T_{gdr}	342°F
Temperature at which property to be measured, T	156.2°F
Room temperature, T_0	70°F
Fiber Volume Fraction, V_f	0.52
Beam Height, h	100 mm
Beam length, L	1000 mm
Beam width, w	200 mm
Plate Hight, h	100 mm
Plate length, L	1000 mm
Plate width, w	1000 mm

4.1

Compos ite Beam

Fi
gures 4.1
presents
one of the
cases of
the
composite
beam
modeled
and
solved in
ANSYS.

The cantilever beam is loaded at its free end by a concentrated force. It can be seen that the deflection of the beam increases continuously until reaching maximum value at the end point of the beam (at the load point).

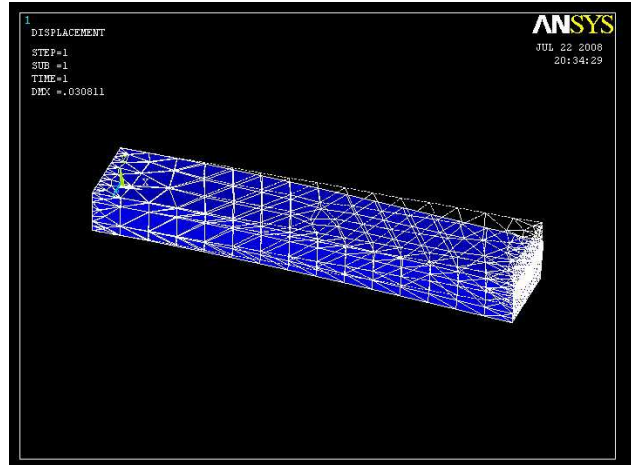


Figure 4.1 Composite beam deflection

From figure 4.2 it can easily be noticed that the horizontal deflection increases continuously until reaching maximum value at the end point of the beam, and it does not have constant values in the same vertical line except at the beginning of the beam (at the fixed point) where the horizontal deflection is almost zero and it is increases vertically at other regions.

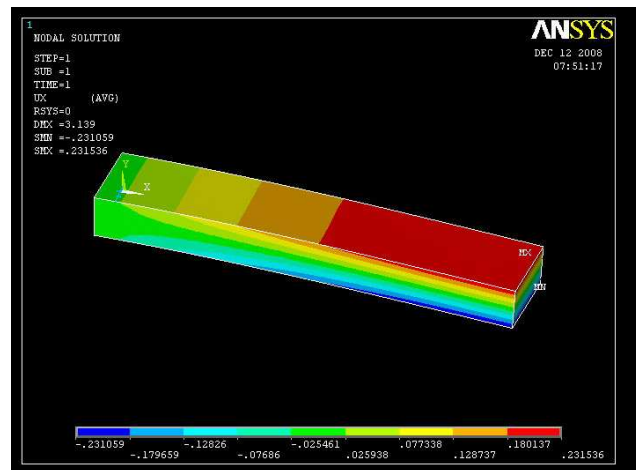


Figure 4.2 Composite beam horizontal deflection

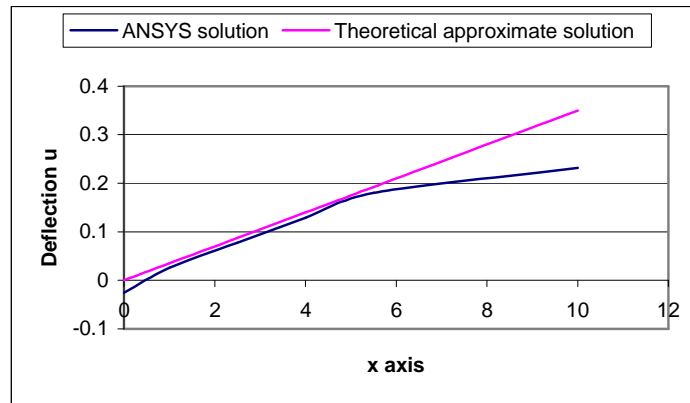


Figure 4.3 Composite beam horizontal deflection curve

A comparison between the finite element solution and the approximate theoretical solution for the horizontal deflection is shown in Fig. 4.3. The agreement between the two methods varies according to the location of the solution. It is important to remember here that the theoretical solution is approximate and needs more refinement through considering more terms in the governing equations.

From figures 4.4 and 4.5 the vertical deflection increases continuously (but with negative values) until reaching maximum value at the end point of the beam, and it has constant values in the same vertical line.

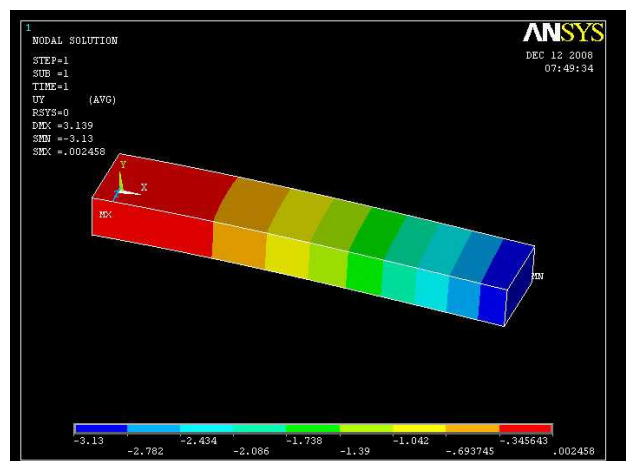


Figure 4.4 Composite beam vertical deflection

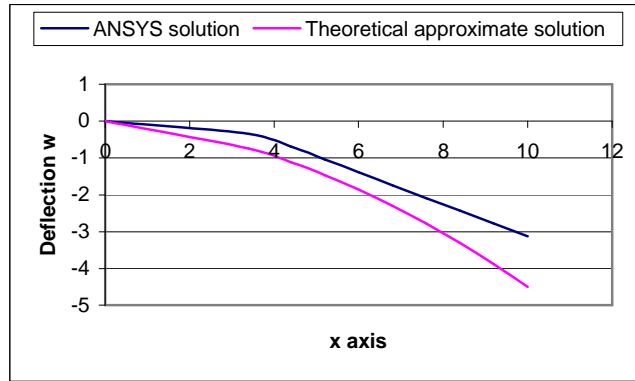


Figure 4.5 Composite beam vertical deflection curve

From figures 4.6 and 4.7 the stresses decreases continuously from its maximum value at the beginning point of the beam , and it does not have constant values in the same vertical line except at the end of the beam where the horizontal deflection is almost zero and it is increases vertically at other regions.

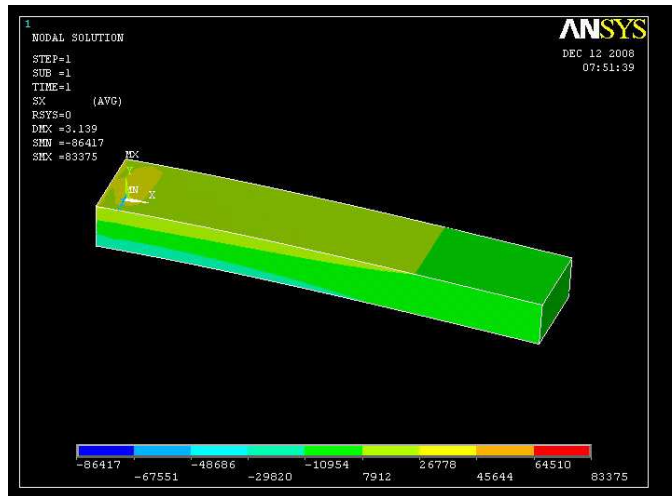


Figure 4.6 Composite beam stresses

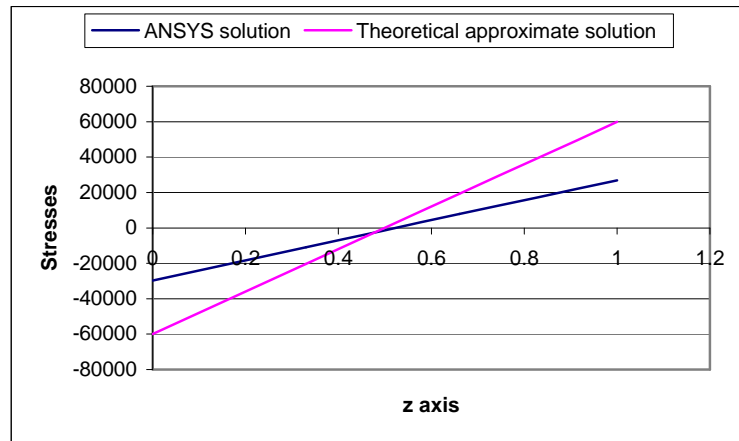


Figure 4.7 Composite beam stresses curve

4.2 Piezoelectric Composite Beam

From figures 4.8 and 4.9 the horizontal deflection increases continuously until reaching maximum value at the end point of the beam, and it does not have constant values in the same vertical line except at the beginning of the beam (at the fixed point) where the horizontal deflection is almost zero and it is increases vertically at other regions. And the deflection increased in this case.

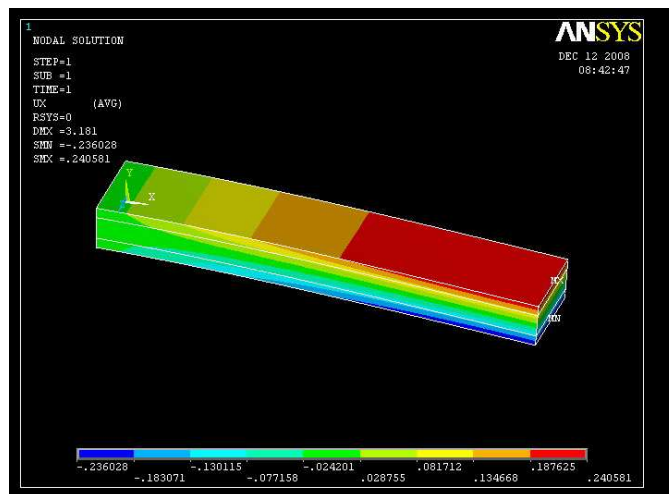


Figure 4.8 Piezoelectric composite beam horizontal deflection

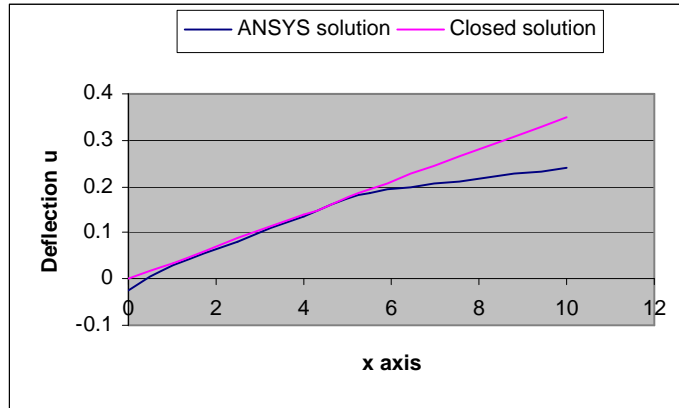


Figure 4.9 Piezoelectric composite beam horizontal deflection curve

From figures 4.10 and 4.11 the vertical deflection increases continuously (but with negative values) until reaching maximum value at the end point of the beam, and it has constant values in the same vertical line. And the deflection increased in this case.

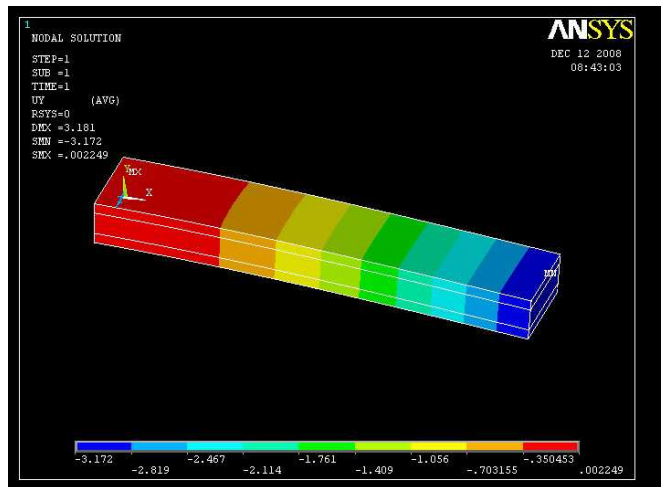


Figure 4.10 Piezoelectric composite beam vertical deflection

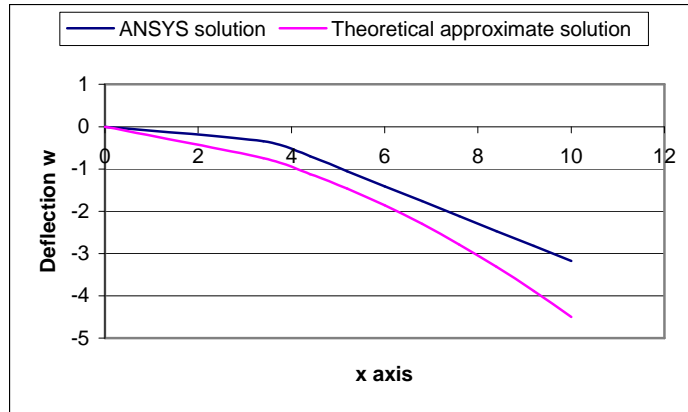


Figure 4.11 Piezoelectric composite beam vertical deflection curve

From figures 4.12 and 4.13 the stresses increases continuously from its minimum value at the bottom point of the beam , and it does not have constant values in the same vertical line except at the end of the beam where the horizontal deflection is almost zero and it is increases vertically at other regions. And the stresses increases in this case.

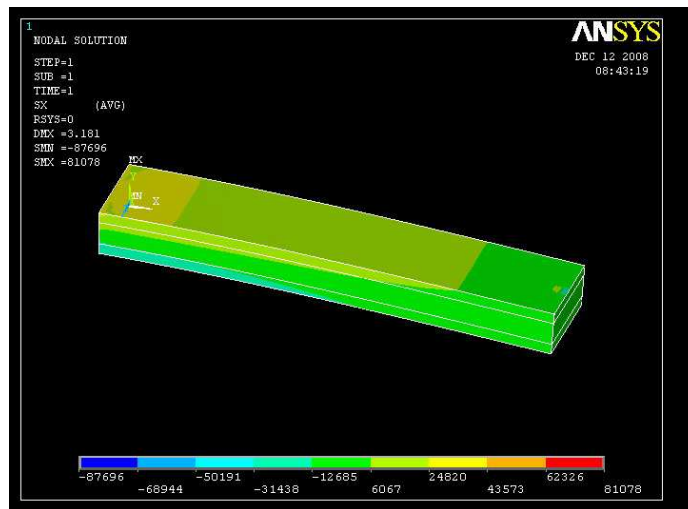


Figure 4.12 Piezoelectric composite beam stresses

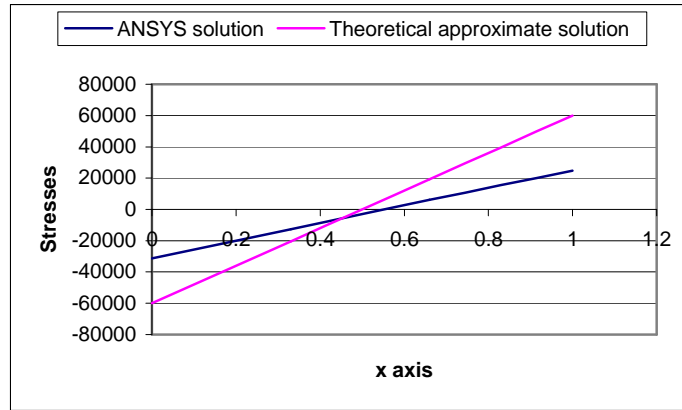


Figure 4.13 Piezoelectric composite beam stresses curve

From figure 4.14 the induced voltage increases continuously until reaching maximum value at the upper point of the piezoelectric layer,

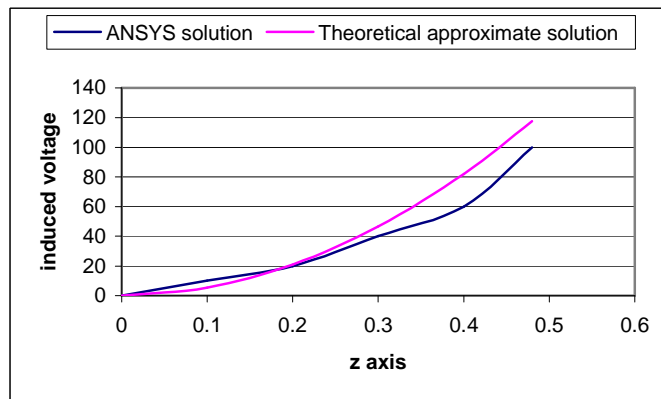


Figure 4.14 Piezoelectric composite beam induced voltage curve

4.3 Hygrothermal Piezoelectric Composite Beam

From figures 4.15 and 4.16 the horizontal deflection increases continuously until reaching maximum value at the end point of the beam, and it does not have constant values in the same vertical line except at the beginning of the beam (at the fixed point) where the horizontal deflection is almost zero and it is increases vertically at other regions. And the deflection increased in this case.

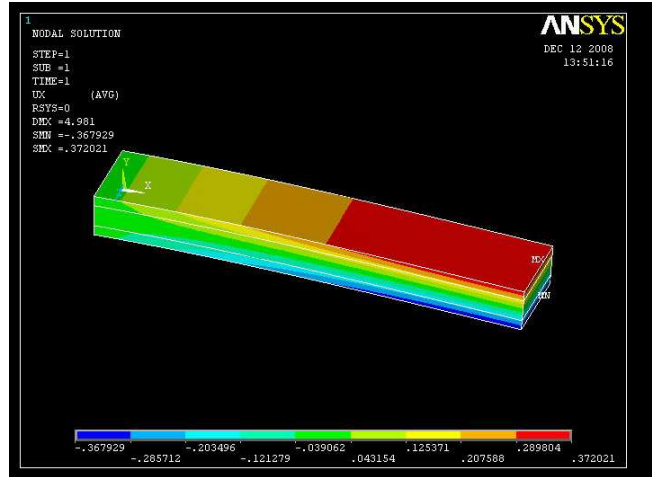


Figure 4.15 Hygrothermal piezoelectric composite beam horizontal deflection

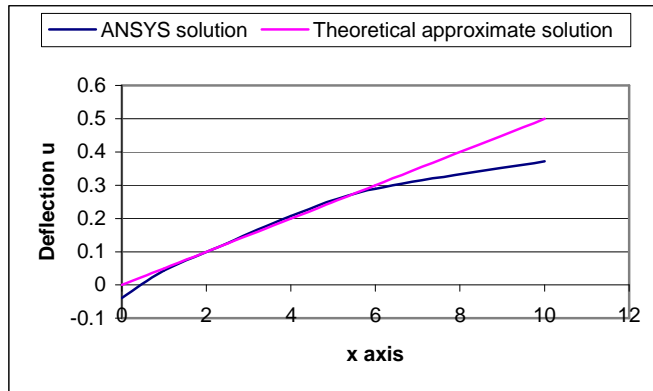


Figure 4.16 Hygrothermal piezoelectric composite beam horizontal deflection curve

From figures 4.17 and 4.18 the vertical deflection increases continuously (but with negative values) until reaching maximum value at the end point of the beam, and it has constant values in the same vertical line. And the deflection increased in this case.

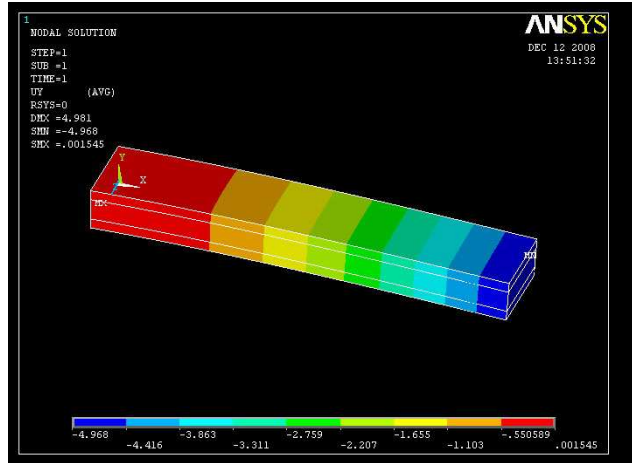


Figure 4.17 Hygrothermal piezoelectric composite beam vertical deflection

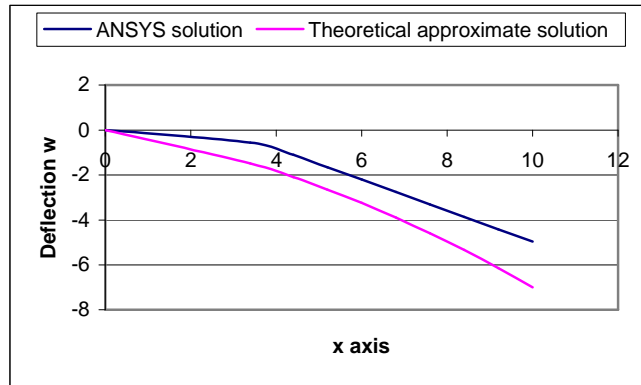


Figure 4.18 Hygrothermal piezoelectric composite beam vertical deflection curve

From figures 4.19 and 4.20 the stresses increases continuously from its minimum value at the bottom point of the beam , and it does not have constant values in the same vertical line except at the end of the beam where the horizontal deflection is almost zero and it is increases vertically at other regions. And the stresses increases in this case.

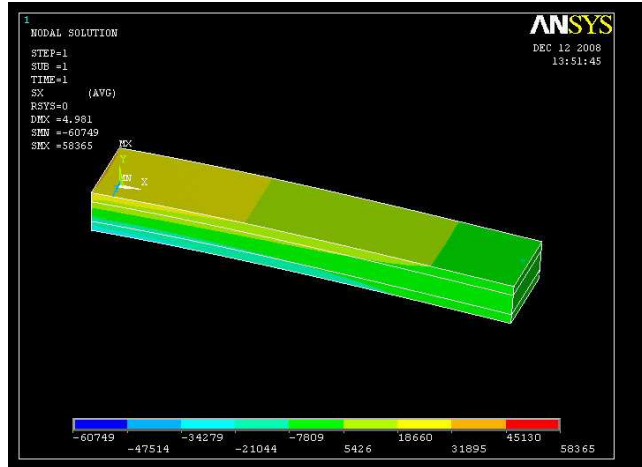


Figure 4.19 Hygrothermal piezoelectric composite beam stresses

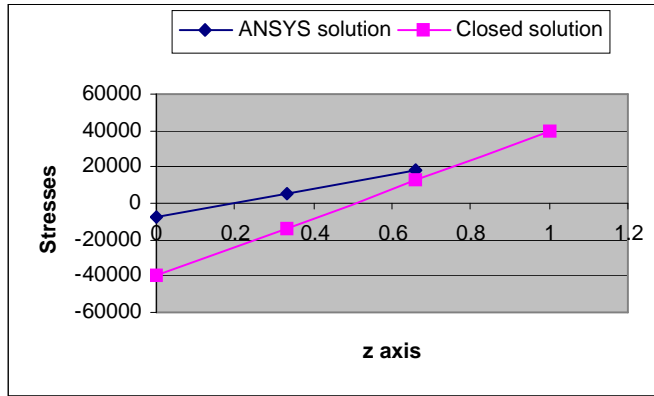


Figure 4.20 Hygrothermal piezoelectric composite beam stresses curve

From figure 4.21 we can note that the horizontal deflection of a hygrothermal piezoelectric beam has a maximum value at $m = 5\%$ and it increases continuously.

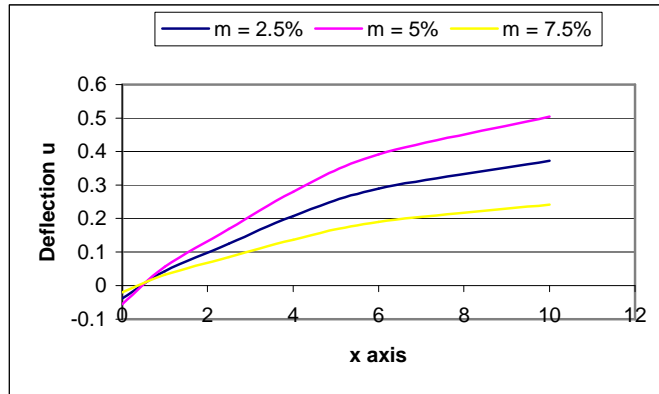


Figure 4.21 Comparison between horizontal deflection values in Hygrothermal piezoelectric composite beam at different moisture values

From figure 4.22 we can note that the vertical deflection of a hygrothermal piezoelectric beam has a maximum value at $m = 5\%$ and it is decreases continuously.

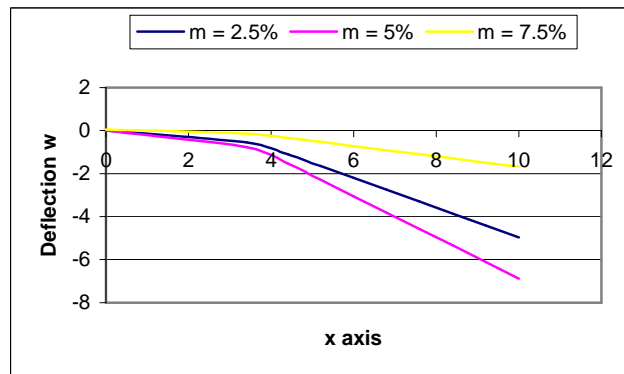


Figure 4.22 Comparison between vertical deflection values in Hygrothermal piezoelectric composite beam at different moisture values

From figure 4.22 we can note that the stresses of a hygrothermal piezoelectric beam has a maximum value at $m = 5\%$ and it is increases continuously.

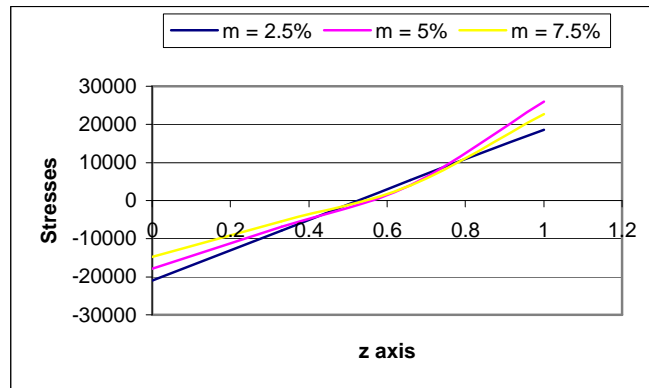


Figure 4.23 Comparison between stress values in Hygrothermal piezoelectric composite beam at different moisture values

The induced voltage does not affected by hygrothermal effects because fiber properties do not affected by these conditions.

4.3 Composite Plate

Same results can be derived for composite plate and same changes will occur with piezoelectric and hygrothermal effects. The following figures present the complete results for the composite plate. Two edges are constrained at all DOF and the other edges are free. The material properties of the plate are entered in the form of modulus of rigidity, Poisson's ratio and young's modulus. Results obtained for this case are similar to those obtained for the beam case.

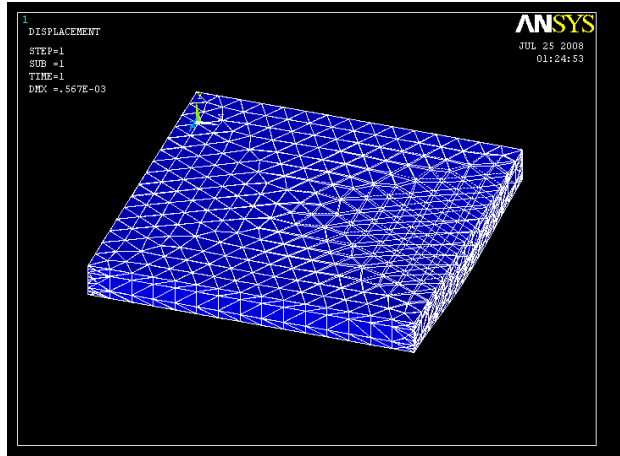


Figure 4.24 composite plate deflection

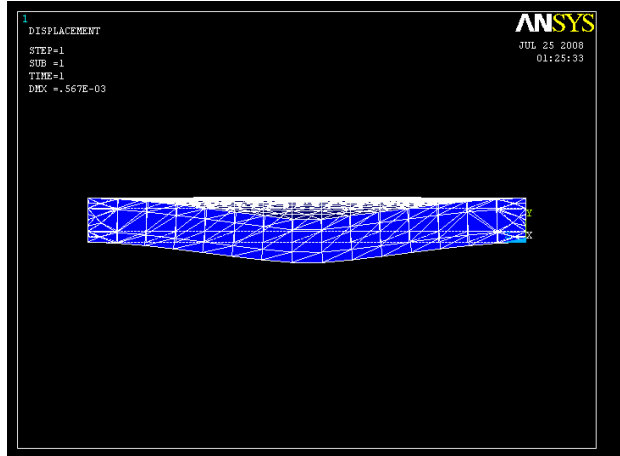


Figure 4.25 composite plate deflection (side view)

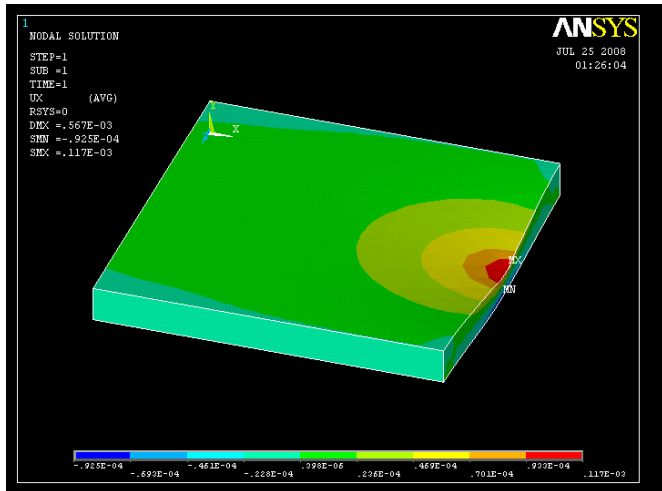


Figure 4.26 composite plate horizontal deflection

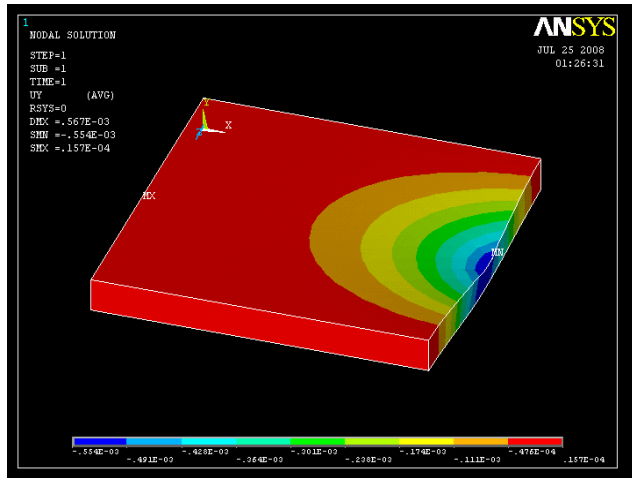


Figure 4.27 composite plate vertical deflection

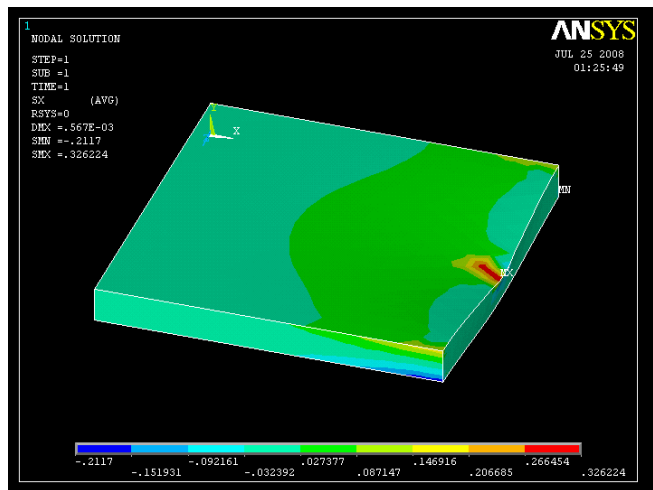


Figure 4.28 composite plate stresses

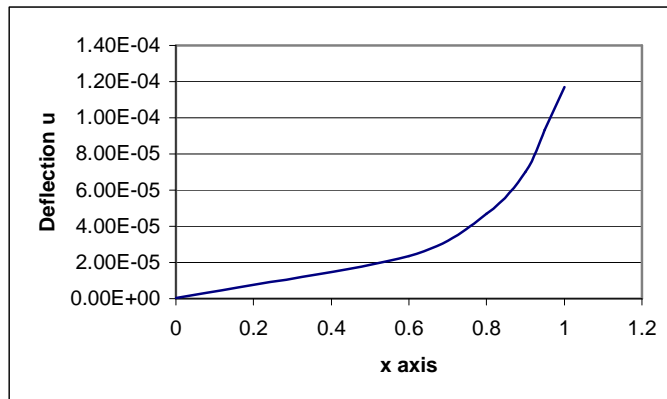


Figure 4.29 composite plate horizontal deflection curve

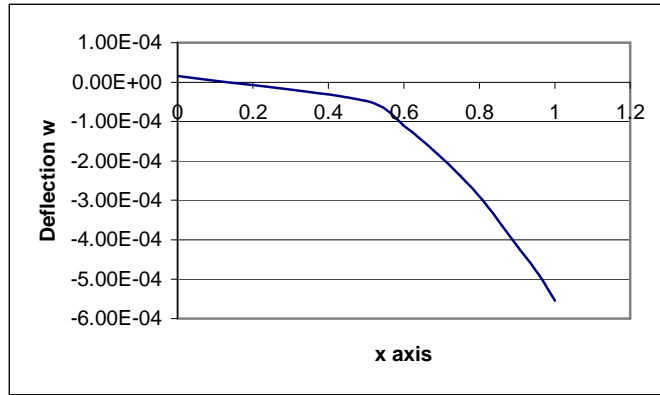


Figure 4.30 composite plate vertical deflection curve

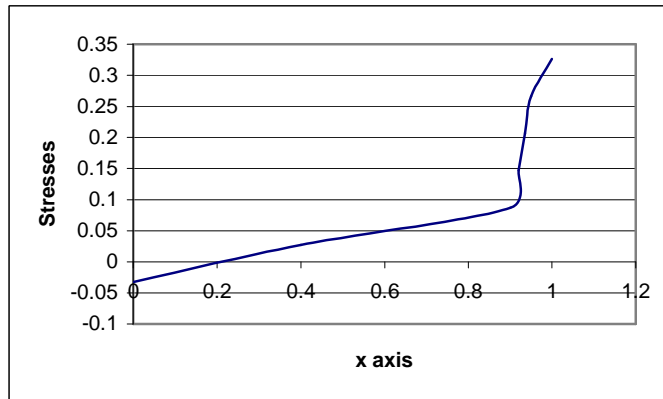


Figure 4.31 composite plate stresses curve

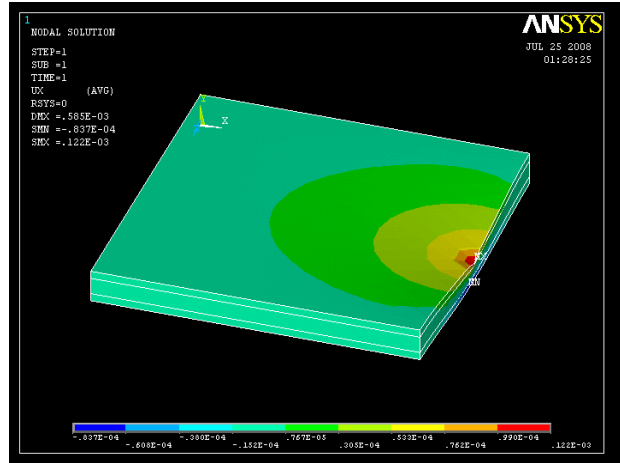


Figure 4.32 Piezoelectric composite plate horizontal deflection

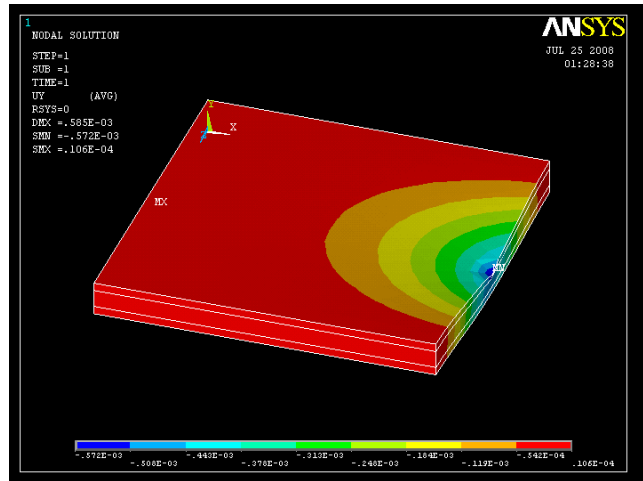


Figure 4.33 Piezoelectric composite plate vertical deflection

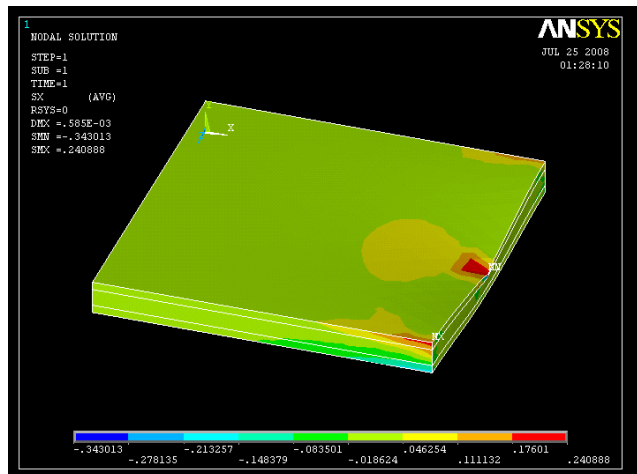


Figure 4.34 Piezoelectric composite plate stresses

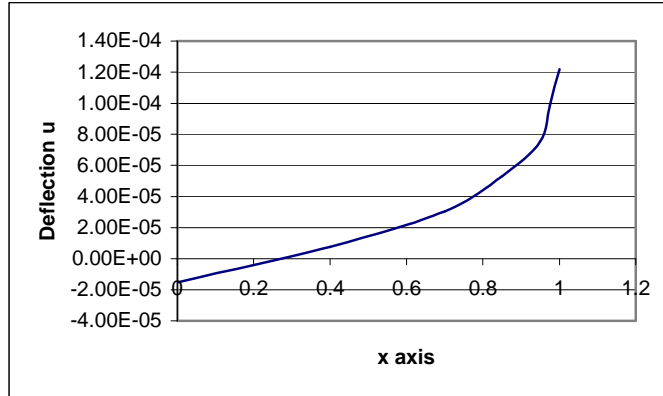


Figure 4.35 Piezoelectric composite plate horizontal deflection curve

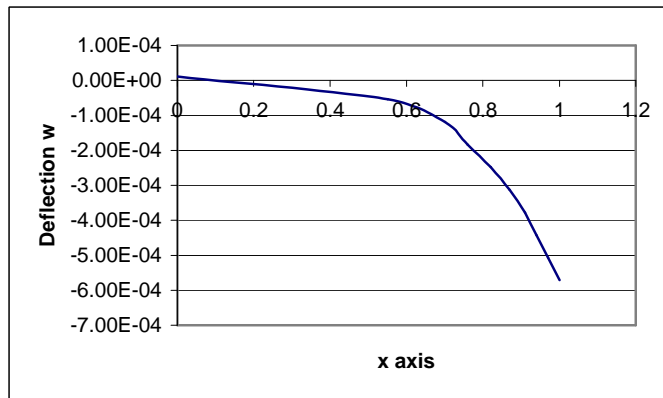


Figure 4.36 Piezoelectric composite plate vertical deflection curve

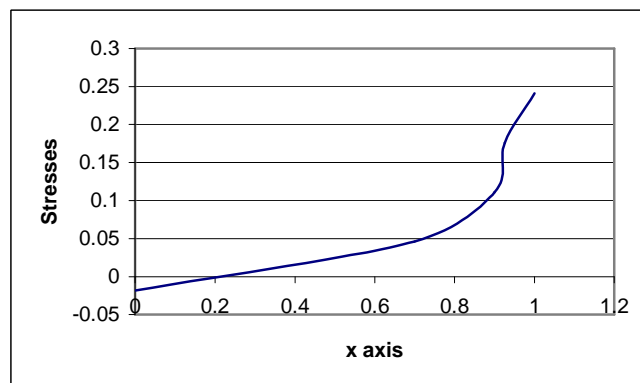


Figure 4.37 Piezoelectric composite plate stresses curve

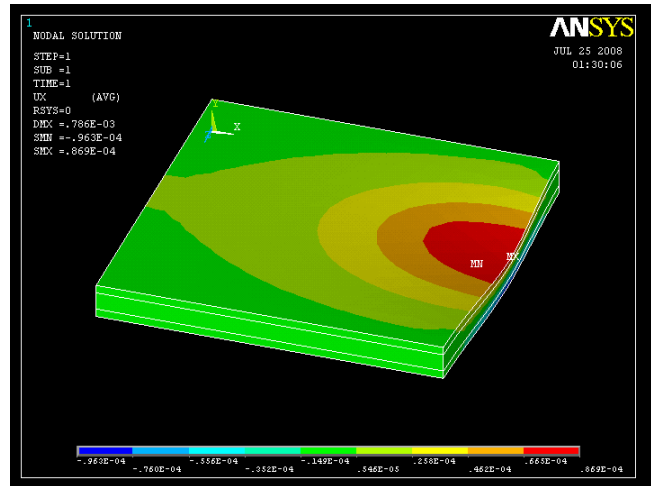


Figure 4.38 Hygrothermal piezoelectric composite plate horizontal deflection

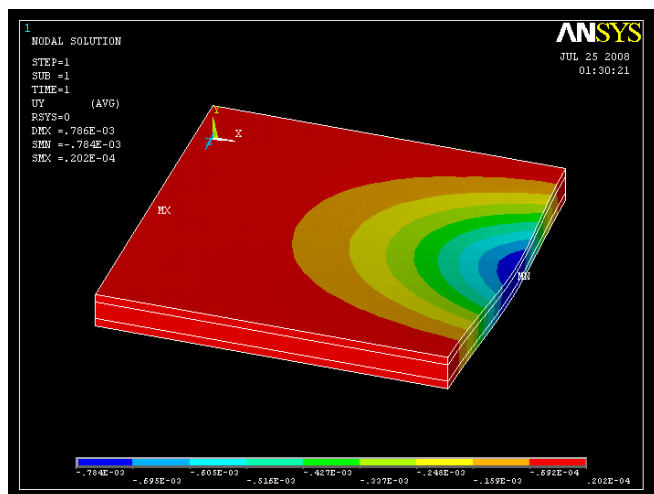


Figure 4.39 Hygrothermal piezoelectric composite plate vertical deflection

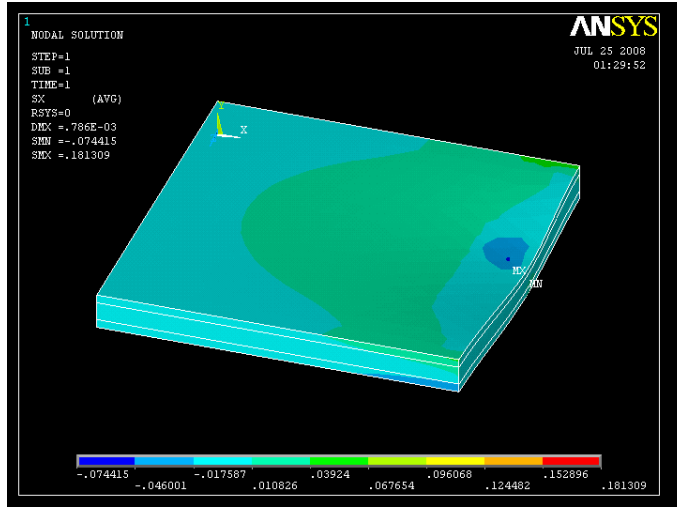


Figure 4.40 Hygrothermal piezoelectric composite plate stresses

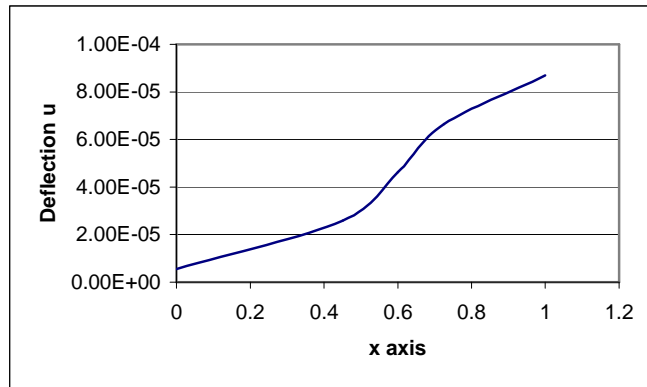


Figure 4.41 Hygrothermal piezoelectric composite plate horizontal deflection curve

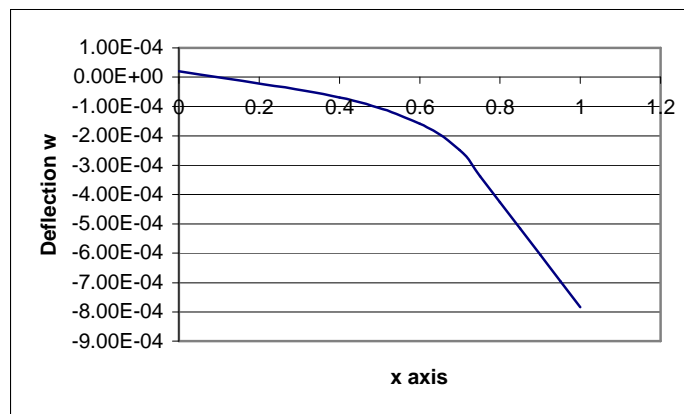


Figure 4.42 Hygrothermal piezoelectric composite plate vertical deflection curve

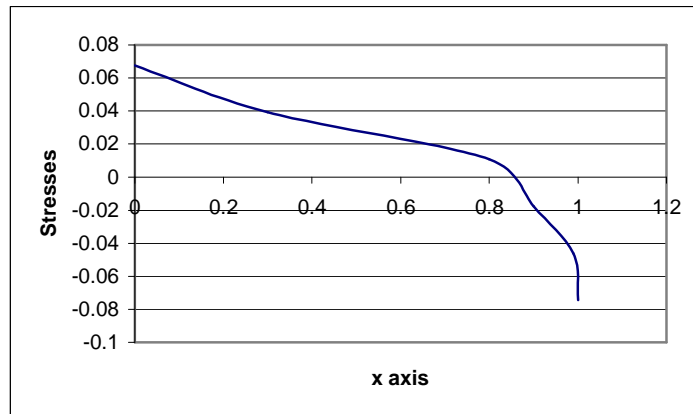


Figure 4.43 Hygrothermal piezoelectric composite plate stresses curve

5 CONCLUSIONS AND RECOMMENDATIONS

5.1 Conclusions

This work investigated the response of piezoelectric beam and plate structures to hygrothermal loading. The interactions between voltage, deflections and stresses are investigated in these structures. Finite element technique is used to model the structures under consideration. Theoretical approximate solution is proposed based on the elastic analysis of the classical lamination theory.

Based on the linear theory of elasticity and piezoelectricity, the exact solutions of the 2D composite beam and piezoelectric composite beam and hygrothermal piezoelectric composite beam are obtained by introducing several formulae. The present results are valid under both plane stress and plane strain conditions and have a good agreement with ANSYS numerical results. Because the piezoelectric coefficient and thickness for various layers can be different in the present investigation, the present work makes it convenient to

model and design different piezoelectric cantilever sensors and actuators. Also ANSYS numerical results are obtained for composite plate with two edges constrained at all DOF and the other edges are free and piezoelectric plate and hygrothermal piezoelectric plate. Different moisture contents are considered and compared.

5.2 Recommendations

- **Exact solution for hygrothermal piezoelectric plate can be obtained. The results can be compared with the numerical results.**
- **Variable load analysis can be performed on the beams. The results can be compared with the present study.**
- **Nonlinear analysis based on large deflection theory may be adopted.**

REFERENCES

- Balasubramanian Datchanamourty 2004 develops a mixed finite element model for composite plates. **University of Kentucky, Lexington, KY 40506-0281**
- B. L. Wang, and N. Noda (2001). Thermally induced fracture of a smart functionally graded composite structure. **Theoretical and Applied Fracture Mechanics 35 (2001) 93-109.**
- B. P. Patel, M. Ganapathi, and D.P. Makhecha (2002). Hygrothermal effects on the structural behaviour of thick composite laminates using higher-order theory. **Institute of Armament Technology, Girinagar, Pune 411 025, India.**
- G Song, X Zhou, and W Binienda (2003). Thermal deformation compensation of a composite beam using piezoelectric actuators. **Smart Mater. Stuct. 13 (2004) 30-37.**
- Jin H. Huang and Yu-Cheng Liu (2006). Electroelastic Response of a Laminated Composite Plate with Piezoelectric Sensors and Actuators. **Journal of Engineering Mechanics. August 2006.**

Jinquan Cheng, Biao Wang, and Shan-Yi Du (2005). A theoretical analysis of piezoelectric/composite anisotropic laminate with larger amplitude deflection effect. **International Journal of Solids and Structures** 42 (2005) 6166-6180.

Ping Tan, and Liyong Tong (2001). Micromechanics models for non-linear behavior of piezoelectric fiber reinforced composite materials. **International Journal of Solids and Structures** 38 (2001) 8999-9032.

Ping Tan, and Liyong Tong (2002). A one-dimensional model for non-linear behavior of piezoelectric composite materials. **Composite Structures** 85 (2002) 551-561.

Praveen Kumar Kavipurapu 2005 The dynamic response of simply supported glass/epoxy composite beams subjected to moving loads in a hygrothermal environment. **Department of Mechanical and Aerospace Engineering**.

Shih-Nung Chen, Gou-Jen Wang, and Ming-Chun Chien (2006). Analytical modeling of piezoelectric vibration-induced micro power generator. **Mechatronics** 16 (2006) 739-387.

S.K. Panda a, and B. Pradhan (2006). Thermoelastic analysis of the asymmetries of interfacial embedded delamination characteristics in laminated FRP composites. **Composites Part A** 38 (2007) 337-347.

S Raja, P K Sinha, G Prathap, and D Dwarakanathan (2004). Thermally induced vibration control of composite plates and shells with piezoelectric active damping. **Journal of Sound and Vibration** 278 (2004) 257-283.

S Raja, P K Sinha, G Prathap, and D Dwarakanathan (2004). Influence of active stiffening on dynamic behaviour of piezo-hygrothermo- elastic composite plates and shells. **Smart Mater. Stuct.** 13 (2004) 939-950.

Y. K. Cheung, and C. P. Jiang (2001). Finite layer method in analysis of piezoelectric composite laminates. **Comput. Methods Appl. Mech. Engrg.** 191 (2001) 879-901.

Z F Shi, H J Xiang, and B F Spencer Jr (2006). Exact analysis of multi-layer piezoelectric/composite cantilevers. **Smart Mater. Stuct.** 15 (2006) 1447-1458.

دراسة تأثير الرطوبة والحرارة على الجهد الكهربائي والإجهادات المتولدة عن
الإحناءات في الإنشاءات الكهربائية الإجهادية المركبة

إعداد

هاني أحمد علي الدرادكة

المشرف

الأستاذ الدكتور ناصر الحنيطي

ملخص

الاهتمام الرئيسي من هذه الدراسة هو دراسة استجابة الإجهادات المركبة للإنشاءات التي تظهر في شكل علاقة بين الإجهاد الميكانيكية والجهد الكهربائي الذي يطرح شكلاً من أشكال الاقتران بين الخصائص الكهربائية والميكانيكية للمواد. الدراسة شملت الاستجابة العامة لإنشاءات دعامية وصفيحية كهربائية إجهادية لتأثير الحرارة والرطوبة. التفاعلات بين الجهد والانحناءات والإجهادات تم دراستها في هذه الإنشاءات. طريقة العنصر المحدود استخدمت لحل نموذج لإنشاءات قيد الدراسة. النظرية التقريبية هو الحل المقترح على أساس التحليل المرن للنظرية الكلاسيكية التصفيفية.

تتناول الدراسة دعامة أفقية تتكون من عدة طبقات (دعامة مركبة) وفي حالة أخرى تكون الطبقة الوسطى في الدعامة طبقة كهربائية إجهادية ثم يتم دراسة هذا النموذج تحت تأثير الحرارة والرطوبة وذلك اعتماداً على نظرية المرونة والإجهادات المركبة ثنائية الأبعاد. لقد تم اتخاذ سماكة الطبقات وعناصر الإجهادات المركبة كمتغيرات. الدراسة الحالية تعطي حلاً باستخدام هذه المتغيرات بواسطة عدة معادلات. هذا الحل يتم مقارنته بالحل الناتج من الطرق العددية باستخدام برنامج (ANSYS). كما يتم استخلاص هذه النتائج العددية لصفيحة مركبة ومن ثم بإضافة طبقة كهربائية إجهادية في وسط الصفيحة ثم يتم دراسة هذا النموذج تحت تأثير الحرارة والرطوبة.